J. Med. Chem. **1998,** *41,* 1146−1154

Potent Antagonists of Somatostatin: Synthesis and Biology

Simon J. Hocart,* Rahul Jain,† William A. Murphy, John E. Taylor,‡ Barry Morgan,‡ and David H. Coy

Peptide Research Laboratories, Tulane University School of Medicine, New Orleans, Louisiana 70112, and Biomeasure Inc., Milford, Massachusetts 01757

Received October 27, 1997

The search for synthetic analogues of somatostatin (SRIF) which exhibit selective affinities for the five known receptor subtypes (sst_{1-5}) has generated a large number of potent agonist analogues. Many of these agonists display good subtype selectivities and affinities for the subtypes 2, 3, and 5, with very few selective for sst_1 or sst_4. Until the recent report by Bass and co-workers (*Mol. Pharmacol.* **1996**, *50*, 709−715; erratum, *Mol. Pharmacol.* **1997**, *51*, 170), no true antagonists had been discovered, let alone any displaying differential receptor subtype selectivity. In this present study, we explore the effect of this putative L^5,D^6 antagonist motif on various series of somatostatin agonist analogues, both linear and cyclic. It was found that many D^5,L^6 agonists could be converted into competitive antagonists by applying this motif, the most potent of which was H-Nal-cyclo[DCys-Pal-DTrp-Lys-Val-Cys]-Nal-NH_2 (**32**). This antagonist was selective for $hsst_2$ with an affinity of 75 nM and an IC_{50} of 15.1 nM against SRIF-14 in a rat in vitro antagonist bioassay. Receptor-selective somatostatin antagonists should provide valuable tools for characterizing the many important physiological functions of this neuropeptide.

Introduction

The tetradecapeptide somatostatin (SRIF)[1] is a potent regulator of endocrine functions. SRIF inhibits the pituitary secretion of growth hormone, the pancreatic secretion of glucagon and insulin, and the secretion of gastrin from the gut. Additionally, SRIF acts as a neurotransmitter or neuromodulator in the central nervous system and peripheral tissues. These biological effects of SRIF, all inhibitory in nature, are elicited through a series of G protein-coupled, transmembrane receptors, of which five different receptor subtypes have been characterized (sst_{1-5}).[2] These five subtypes have similar affinities for the endogenous SRIF ligands but have differing distributions in various tissues.[3] The development of potent, smaller SRIF agonists led to the discovery of differing affinities of the various shortened ligands for the different subtypes.[4,5] These selective agonists are currently being used to probe the physiological role of each of the receptors,[6−8] but this endeavor would be enhanced by the development of receptor-specific antagonists. Also, SRIF antagonists might provide a novel route to increasing endogenous levels of some hormones, notably growth hormone and insulin.

Some years ago, we reported the first partial antagonist of somatostatin: cyclo(Ahp-Phe-DTrp-Lys-Thr-(Bzl)).[9] This analogue (JLF-3-14, BIM-23156) was a weak antagonist at low doses, stimulating growth in female rats,[10] but was an agonist at higher doses, although the analogue does not bind to cloned human sst receptors (see Table 3). However, a recent observation by Bass and co-workers has appeared to realize the goal of pure antagonists.[12,13] They noted that a weak linear octapeptide agonist we reported recently[5] had a high affinity for sst_2 and thus was a good candidate from which to derive an antagonist. They designed disulfide-cyclized analogues employing inverted chirality in positions 5 and 6 relative to the agonists. These compounds were shown to antagonize the action of SRIF in a cAMP accumulation assay and the somatostatin-stimulated growth of yeast cell expressing the sst_2 subtype. Of these antagonists, Ac-Npa^5-cyclo(DCys^6-Tyr^7-DTrp^8-Lys^9-Thr^{10}-Cys^{11})-DTyr^{12}-NH_2 (SRIF numbering) had an affinity for sst_2 comparable with the native hormone.[11,12] In this paper, we further explore this observation by applying this structural motif to some of our SRIF analogues.

Results and Discussion

The search for synthetically facile analogues of SRIF has demonstrated that only two amino acids (DTrp^8-Lys^9) are required for full receptor recognition and bioactivity.[12−14] These crucial amino acids form part of a β-bend which is usually stabilized via cyclization of the backbone, a disulfide bridge, or both constraints.[15,16] The effect of changes in the endocyclic bridging region on biological activity has been probed by the insertion of proline analogues of varying ring sizes,[17] by modification of the sulfur bridge of cystine to monosulfide[17] and trisulfide moieties,[18] and by side chain−side chain cyclization.[19] In further exploring the structure−activity relationships of somatostatin analogues, we have described a new series of selective linear analogues which contain aromatic residues in place of the more usual cystine bridge.[5] As supported by low-temperature NMR studies, these linear compounds maintain the conformation of the β-bend through hydrophobic interactions of the aromatic side chains.[20] In most of these analogues, residues at position 5 are in the D configuration with position 6 in the L configuration. We have

‡ Biomeasure Inc.

† Current address: Department of Medicinal Chemistry, National Institute of Pharmaceutical Education and Research, Sector 67, S.A.S. Nagar (Mohali), 160062 India.

S0022-2623(97)00730-9 CCC: $15.00
Published on Web 03/06/1998

Table 1. Amino Acid Sequences of the Analogues

analogue number	analogue code	peptide structure
1	RJ-01-48	cyclo[NMeDAla-Tyr-DTrp-Lys-Val-Phe]
2	NC-11-31	H-Ala-Gly-cyclo[Cys-Lys-Asn-DPhe-Phe-DTrp-Lys-Thr-Phe-Thr-Ser-Cys]-OH
3	DC-38-28	H-Phe-DPhe-Tyr-DTrp-Lys-Thr-Phe-Thr-NH_2
4	DC-38-25	H-DPhe-DPhe-Tyr-DTrp-Lys-Thr-Phe-Thr-NH_2
5	DC-38-45	H-Phe-DCpa-Tyr-DTrp-Lys-Val-Phe-Thr-NH_2
6	DC-38-42	H-Nal-DCpa-Tyr-DTrp-Lys-Val-Phe-Thr-NH_2
7	DC-32-15	H-DNal-DCpa-Tyr-DTrp-Lys-Val-Phe-Thr-NH_2
8	DC-38-73	H-Nal-DCpa-Tyr-DTrp-Lys-Val-Phe-Nal-NH_2
9	DC-38-76	H-DNal-DCpa-Tyr-DTrp-Lys-Val-Phe-Nal-NH_2
10	DC-38-58	H-Nal-cyclo[DCys-Tyr-DTrp-Lys-Val-Cys]-Thr-NH_2
11	BIM-23246	H-DNal-cyclo[DCys-Tyr-DTrp-Lys-Val-Cys]-Thr-NH_2
12	DC-38-61	(NH_2)-Phe-cyclo[DCys-Tyr-DTrp-Lys-Val-Cys]-Thr-NH_2
13	DC-38-55	Ac-cyclo[DCys-Tyr-DTrp-Lys-Val-Cys]-Thr-NH_2
14	BIM-23255	H-DNal-cyclo[Cys-Tyr-DTrp-Lys-Val-DCys]-Thr-NH_2
15	JF-04-31	H-DPhe-cyclo[DCys-Tyr-DTrp-Lys-Abu-Cys]-Thr-NH_2
16	DC-13-187	H-DPhe-cyclo[DPen-Tyr-DTrp-Lys-Val-Cys]-Thr-NH_2
17	DC-13-209	H-DPhe-cyclo[Cys-Tyr-DTrp-Lys-Val-DPen]-Thr-NH_2
18	DC-38-19	H-Phe-cyclo[DCys-Pal-DTrp-Lys-Thr-Cys]-Thr-NH_2
19	DC-38-22	H-DPhe-cyclo[DCys-Pal-DTrp-Lys-Thr-Cys]-Thr-NH_2
20	DC-38-15	H-Tyr-cyclo[DCys-Pal-DTrp-Lys-Thr-Cys]-Thr-NH_2
21	DC-38-39	H-Nal-cyclo[DCys-Tyr-DTrp-Lys-Val-Cys]-Nal-NH_2
22	DC-38-35	Ac-Nal-cyclo[DCys-Tyr-DTrp-Lys-Val-Cys]-Nal-NH_2
23	DC-32-57	H-DNal-cyclo[DCys-Tyr-DTrp-Lys-Val-Cys]-Nal-NH_2
24	DC-38-67	H-Nal-cyclo[DCys-Tyr-DTrp-Lys-Val-Cys]-DNal-NH_2
25	DC-38-64	H-DNal-cyclo[DCys-Tyr-DTrp-Lys-Val-Cys]-DNal-NH_2
26	NC-8-61	H-DNal-cyclo[DCys-Tyr-DTrp-Lys-Thr-Cys]-Nal-NH_2
27	DC-32-53	H-DNal-cyclo[Cys-Tyr-DTrp-Lys-Val-DCys]-Nal-NH_2
28	DC-38-70	H-Trp-cyclo[DCys-Tyr-DTrp-Lys-Val-Cys]-DNal-NH_2
29	JF-04-47	H-DBip-cyclo[DCys-Tyr-DTrp-Lys-Val-Cys]-Nal-NH_2
30	RJ-01-14	H-Nal-cyclo[DCys-Tyr-DTrp-Lys-Val-Cys]-NHCH(CH_3)$_2$
31	RJ-01-20	H-Nal-cyclo[DCys-His-DTrp-Lys-Val-Cys]-Nal-NH_2
32	DC-38-48	H-Nal-cyclo[DCys-Pal-DTrp-Lys-Val-Cys]-Nal-NH_2
33	DC-38-51	H-Phe-cyclo[DCys-Pal-DTrp-Lys-Val-Cys]-Nal-NH_2
34	RJ-01-28	H-Dip-cyclo[DCys-Pal-DTrp-Lys-Val-Cys]-Nal-NH_2
35	RJ-01-44	H-Dip-cyclo[DCys-Pal-DTrp-Lys-Val-Cys]-Nal-NH_2
36	RJ-01-76	H-Dip-cyclo[DCys-Pal-DTrp-Lys-Val-Cys]-Dip-NH_2
37	RJ-01-31	H-Dip-cyclo[DCys-His-DTrp-Lys-Val-Cys]-Dip-NH_2
38	RJ-01-36	H-Dip-cyclo[DCys-His-DTrp-Lys-Val-Cys]-Nal-NH_2
39	RJ-01-40	H-Nal-cyclo[DCys-His-DTrp-Lys-Val-Cys]-DDip-NH_2
40	RJ-01-80	H-Nal-cyclo[DCys-Pal-DTrp-Lys-Val-Cys]-Dip-NH_2
41	DC-37-57	H-cyclo[DCys-Phe-Phe-DTrp-Lys-Thr-Phe-Cys]-NH_2
42	DC-37-83	H-cyclo[DCys-Phe-Phe-DTrp-Lys-Thr-Phe-DCys]-NH_2
43	JF-04-33	H-Npa-cyclo[DCys-Pal-DTrp-Lys-Val-Cys]-Tyr-NH_2
44	JF-04-27	H-Npa-cyclo[DCys-Tyr-DTrp-Lys-Val-Cys]-Tyr-NH_2

synthesized several compounds to explore the effect of the inversion of the chirality of these residues on binding to different subtypes of the cloned human receptors and on the antagonism of SRIF-inhibited growth hormone release in the rat (see Table 1).

Cyclic Hexapeptide. One of the smallest reported SRIF analogues is the hexapeptide superagonist MK-678 (Seglitide).[16] Inversion of the chirality of NMeAla^6 in MK-678 gave compound **1** (RJ-01-48; see Table 1),[18] an agonist with a reasonable affinity for sst_2 but no antagonist activity at the doses tested.[21] This was not unexpected since these structurally minimized superagonists are highly refined and thus are poor targets for modification. We also tried this modification in the native tetradecapeptide hormone (DPhe^6-DTrp^8-SRIF; compound **2**, NC-11-31), but the binding affinity for each receptor subtype was markedly lowered, although it bound selectively to sst_2. At the doses investigated, the analogue had no antagonist activity.

Linear Octapeptides. Although SRIF is a cyclic peptide and most of the smaller analogues described have also been cyclic encompassing various ring sizes and cyclization strategies, we recently developed a series of linear analogues with good selectivity for the receptor subtypes sst_2, sst_3, and sst_5.[4,5] To investigate the effect of the putative antagonist motif in the linear analogues, we synthesized several linear sequences with inverted chirality in positions 5 and 6 based on these analogues (compounds **3**−**9**; see Table 1). Compound **3** (DC-38-28) and its DPhe^5 isomer **4** (DC-38-25) both had poor affinity for each subtype and were inactive in the antagonist assay at the doses tested. Substitution of DCpa^6 and Val^{10} to produce a more hydrophobic analogue reduced the affinities further and gave an inactive compound at the doses tested (**5**, DC-38-45). However, the further substitution of the large hydrophobic aromatic moiety Nal in position 5 (**6**, DC-38-42) produced a weak antagonist with an IC_{50} of 3.03 μM, though with poor affinity for sst_2 (706 nM). Inversion of this moiety to DNal^5 (**7**, DC-32-15) retained the antagonism but markedly increased the affinity for sst_2, sst_3, and sst_5. Substituting the bulky hydrophobic residue Nal for Thr at the carboxyl terminus together with either Nal^5 or DNal^5 (compounds **8**, DC-38-73, and **9**, DC-38-76, respectively) produced a marked reduction in both affinity and antagonism.

Octapeptides Containing a Cyclic Hexapeptide Core. In the case of the octapeptides cyclized between

Table 2. Analytical Data on the Compounds

analogue number	analogue code	mass spectrum M − H$^+$		HPLC−1[a]		HPLC−2[b]	
		calcd[c]	obsd[d]	t_R (min)	purity (%)	t_R (min)	purity (%)
1	RJ-01-48	810.0	810.4	32.34	99	32.85	99
2	NC-11-31	1638.9	1637.8	31.83	97	31.33	97
3	DC-38-28	1139.3	1140.3	33.99	99	33.21	99
4	DC-38-25	1139.3	1139.8	29.98	99	28.88	99
5	DC-38-45	1171.8	1172.0	40.06	99	39.38	99
6	DC-38-42	1221.9	1222.2	44.18	98	43.33	99
7	DC-32-15	1221.9	1223.0	42.60	98	41.48	98
8	DC-38-73	1318.0	1320.7	54.18	97	52.52	99
9	DC-38-76	1318.0	1321.7	49.98	99	47.40	98
10	DC-38-58	1097.4	1097.6	29.79	97	29.07	97
11	BIM-23246	1097.4	1097.7	31.32	99	29.79	99
12	DC-38-61	1032.2	1032.3	32.54	98	32.95	99
13	DC-38-55	942.1	942.5	21.78	98	22.37	99
14	BIM-23255	1097.4	1097.3	28.70	99	27.06	99
15	JF-04-31	1033.2	1033.5	22.98	99	21.45	99
16	DC-13-187	1076.3	1075.9	30.13	97	29.20	99
17	DC-13-209	1076.3	1076.0	26.40	99	25.00	99
18	DC-38-19	1034.2	1033.4	14.22	99	12.43	99
19	DC-38-22	1034.2	1034.9	15.26	99	13.46	99
20	DC-38-15	1050.2	1050.6	11.01	99	9.41	99
21	DC-38-39	1193.5	1193.7	39.11	97	38.16	97
22	DC-38-35	1235.6	1235.4	44.33	97	44.48	97
23	DC-32-57	1193.5	1193.5	40.03	99	39.03	97
24	DC-38-67	1193.5	1193.6	41.70	99	40.78	99
25	DC-38-64	1193.5	1193.6	40.72	98	39.47	98
26	NC-8-61	1195.5	1195.4	35.78	97	34.84	97
27	DC-32-53	1193.5	1194.6	38.52	97	37.25	97
28	DC-38-70	1182.5	1182.8	39.30	99	37.64	97
29	JF-04-47	1219.5	1219.2	41.94	98	41.09	97
30	RJ-01-14	1038.3	1037.4	39.43	99	38.08	99
31	RJ-01-20	1167.5	1168.2	32.72	98	30.79	98
32	DC-38-48	1178.5	1178.7	33.23	97	35.11	98
33	DC-38-51	1128.4	1128.7	29.73	97	32.27	97
34	RJ-01-28	1204.5	1206.1	34.19	99	35.65	98
35	RJ-01-44	1204.5	1204.6	33.89	97	37.98	97
36	RJ-01-76	1230.5	1230.2	35.73	99	37.67	99
37	RJ-01-31	1219.5	1219.7	35.22	99	33.38	99
38	RJ-01-36	1193.5	1194.0	33.77	99	31.96	99
39	RJ-01-40	1193.5	1193.3	36.37	99	34.00	99
40	RJ-01-80	1204.5	1203.0	35.01	99	37.43	99
41	DC-37-57	1079.3	1080.2	37.68	99	36.82	98
42	DC-37-83	1079.3	1080.1	36.06	99	35.15	99
43	JF-04-33	1139.4	1139.2	20.65	99	21.22	98
44	JF-04-27	1154.4	1157.1	28.13	97	26.61	97

[a] Elution system: A, 0.1% TFA; B, 0.1% TFA in 80% MeCN; 10% B to 70% B at 1% min^{-1} and 1.5 mL min^{-1}. [b] Elution system:C, 5% MeCN in TEAP (0.1 M, pH 3); D, 20% C in MeCN; 0% D to 60% D at 1% min^{-1} and 1.5 mL min^{-1}. [c] Theoretical molecular weight (M − H$^+$, Da). [d] Actual molecular weight (M − H$^+$, Da) observed.

positions 6 and 11, a class which includes some of the most potent agonists[22] with high selectivities for the sst_2 receptor, the presence of hydrophobic amino acids in position 5 with Thr[12] generally leads to high affinities for sst_2 and sst_3 and high GH release-inhibiting potencies.[5,23−25] Inverting the chirality of positions 5 and 6 of BIM-23014 (Lanreotide) reduced the affinity for sst_2 dramatically (compound **10**, DC-38-58) giving an analogue which was inactive in the antagonist assay at the doses tested. The DNal[5] analogue was similarly inactive (**11**, BIM-23246) as was the N$^\alpha$desamino analogue (**12**, DC-38-61).[22] The N$^\alpha$des-Phe[5] analogue (**13**, DC-38-55) lost all binding ability. The reversal of chirality of the bridging cysteines also gave an inactive compound in the antagonism assay at the test doses as expected (14, BIM-23255). The substitution of Abu[10], which was associated with high affinity for sst_2 in some agonists, noticeably increased the affinity for sst_5 (**15**, JF-04-31; K_i 30 nM) but again was inactive at the doses tested. To probe the effects of extra steric bulk on the disulfide bridge, the sterically constrained cysteine analogue penicillamine was also incorporated in positions 6 and 11 (**16**, DC-13-187, and **17**, DC-13-209, respectively), but in the former case, receptor affinity was almost totally abolished. Neither compound was active in the antagonist assay at doses up to 10 μM. (Analytical data are given in Table 2, and binding affinities are listed in Table 3.)

Position 7 in the SRIF analogues is part of the crucial β-bend region and is invariably an aromatic amino acid. In the structure−activity investigations of luteinizing hormone-releasing hormone (LHRH), the replacement of an aromatic amino acid with one containing a pyridine moiety led to enhanced biological activity.[26] In the case of these SRIF analogues, substitution of Tyr[7] with Pal[7] produced an antagonist with an IC_{50} of 905 nM and a marginal affinity for sst_2 (**18**, DC-38-19). The inversion of Phe[5] to DPhe[5] halved the affinity for sst_2 and abolished the antagonism at the test doses (**19**, DC-38-22). Tyr[5] further reduced the receptor affinities but retained some antagonism (**20**, DC-38-15; IC_{50} 98 μM).

Many of the more potent octapeptide agonists of SRIF contain a large aromatic amino acid at the carboxyl terminus. We made a series of analogues containing

Table 3. Binding Affinities for the Cloned Human sst_{1-5} Receptors and Antagonist IC_{50} Data

analogue number	analogue code	$hsst_1$[a] (nM)	$hsst_2$[a] (nM)	$hsst_3$[a] (nM)	$hsst_4$[a] (nM)	$hsst_5$[a] (nM)	antagonist (μM) IC_{50}[b]	SEM	*n*
	SRIF	2.26 ± 0.47	0.23 ± 0.04	1.17 ± 0.28	1.77 ± 0.28	1.41 ± 0.29			
	JLF-3-14	1000	1000	nd[c]	1000	1000	nd		
1	RJ-01-48	1000	7.8 ± 1.6	404 ± 56.3	1000	1000	na[d]		
2	NC-11-31	945	34.7 ± 7.9	539 ± 179	1172	347 ± 178	na[d]		
3	DC-38-28	1000	445 ± 67.8	216 ± 84.0	1000	1176 ± 176	na[d]		
4	DC-38-25	nd	nd	nd	nd	nd	na[d]		
5	DC-38-45	1000	797 ± 82.5	648	1000	2741 ± 992	na[d]		
6	DC-38-42	1000	706 ± 176	1127 ± 127	2844	1837 ± 772	3.03	0.82	4
7	DC-32-15	1000	144 ± 19.0	89.9 ± 37.0	1000	21.6 ± 1.6	3.96	1.55	5
8	DC-38-73	1000	1000	1609	1000	1959 ± 118	63.6	24.80	2
9	DC-38-76	1000	526 ± 203	619	1000	178 ± 71	57.1	33.2	2
10	DC-38-58	2163	118 ± 73.6	733 ± 226	1000	208 ± 78	na[d]		
11	BIM-23246	1580 ± 808	306 ± 134	nd	1000	152	na[d]		
12	DC-38-61	1000	197 ± 112	525 ± 196	1000	1060	na[d]		
13	DC-38-55	1000	1000	1000	1000	1000	na[d]		
14	BIM-23255	4843	350 ± 43	1000	1000	123	na[d]		
15	JF-04-31	1000	183 ± 95	140 ± 93.6	1000	30.3 ± 9.80	na[d]		
16	DC-13-187	1000	2546	821 ± 470	1000	3356 ± 1644	na[e]		
17	DC-13-209	nd	nd	nd	nd	nd	na[e]		
18	DC-38-19	1000	291 ± 14.0	934 ± 190	1000	2359	0.905	0.104	4
19	DC-38-22	1000	566 ± 115	1361 ± 392	1000	1000	na[d]		
20	DC-38-15	1000	1000	1380 ± 531	1000	3700	98.65	85.35	2
21	DC-38-39	2003 ± 231	37.6 ± 8.3	161 ± 13.0	1000	302 ± 40	0.0353	0.0068	4
22	DC-38-35	1025 ± 198	48.2 ± 7.9	144 ± 9.4	1000	130 ± 60	0.0567	0.0351	4
23	DC-32-57	494 ± 301	68.5 ± 23.9	292 ± 100	312 ± 119	744 ± 311	1.36	0.42	3
24	DC-38-67	1000	46.1 ± 9.5	2276 ± 15.7	1000	1247 ± 677	0.280	0.0400	2
25	DC-38-64	1665	82.9 ± 5.0	1076 ± 171	1000	358 ± 127	0.375	0.2150	2
26	NC-8-61	1044	202 ± 93.5	nd	605	290	180		1
27	DC-32-53	1000	139 ± 62.8	1000	1000		na[e]		
28	DC-38-70	588	77.2 ± 17.3	649 ± 224	1000	221 ± 68	0.0648	0.0552	2
29	JF-04-47	1439 ± 439	793 ± 331	466 ± 52.8	1000	243	0.810	0.0300	2
30	RJ-01-14	1000	435 ± 126	1228	1000	470 ± 114	108.6	0.60	2
31	RJ-01-20	1000	82.5 ± 17.3	68	943	501 ± 197	0.053	0.0286	3
32	DC-38-48	506	75.9 ± 13.2	171 ± 45.4	1000	524 ± 175	0.0151	0.0036	5
33	DC-38-51	535	123 ± 25.3	373 ± 38.0	1000	769 ± 253	0.0580	0.0240	2
34	RJ-01-28	495	509 ± 118	314 ± 65.5	1000	302	0.066	0.0184	4
35	RJ-01-44	4599	1348 ± 238	273 ± 101	932	2462	0.335	0.0450	2
36	RJ-01-76	1000	1812	1302 ± 293	1000	2032	0.500	0.1200	2
37	RJ-01-31	1000	669 ± 60.0	1756 ± 421	3007	1484 ± 337	0.975	0.0050	2
38	RJ-01-36	1008 ± 8	824 ± 40.3	435 ± 43.9	1000	1834	0.130	0.0100	2
39	RJ-01-40	1086 ± 86	17.8 ± 1.7	1196 ± 101	1000	1000	0.110	0.0058	3
40	RJ-01-80	1000	355 ± 118	903 ± 491	1000	1000	0.056	0.0232	4
41	DC-37-57	nd	nd	nd	nd	nd	na[e]		
42	DC-37-83	723 ± 94	34.8 ± 5.7	5.6 ± 0.6	406	28.0 ± 14.7	na[e]		
43	JF-04-33	245	35.3 ± 10.3	235 ± 75.1	757 ± 243	529	0.026	0.0075	2
44	JF-04-27	3219	23.4 ± 5.2	177	632	101 ± 41	0.050	0.0179	4

[a] Expressed as the mean ± SEM; single values indicate the results of one binding experiment. [b] Antagonist IC_{50} (μM) versus SRIF (1.0 nM), expressed as the mean and SEM of *n* separate dose−response curves. [c] Not determined. [d] Not an antagonist at doses up to 100 μM. [e] Not an antagonist at doses up to 10 μM.

Nal^{12} based on the moderately active agonist BIM-23042.[27] Substitution of Nal^5 and $DCys^6$ in BIM-23042 gave compound **21** (DC-38-39), which displayed good affinity for sst_2 (37 nM) but also bound fairly well to sst_3 and to a lesser extent to sst_5 (160 and 302 nM, respectively). This compound was an antagonist in rat pituitary cells with an IC_{50} of 35.3 nM. N^{α}-Acetylation increased the affinity for sst_5 but reduced the antagonism IC_{50} to 56.7 nM (**22**, DC-38-35) while adversely affecting solubility. Inversion of position 5 to DNal (**23**, DC-32-57) lowered the antagonist activity substantially to 1.36 μM, while the affinity for sst_2 was only halved. In contrast, the substitution of Nal^5 and $DNal^{12}$ (**24**, DC-38-67) caused a less dramatic loss of antagonism (ca. 10-fold to 280 nM) with little effect on the binding affinity to sst_2 but a complete loss of binding to sst_3 and sst_5 (>1000 nM each). Some affinity for sst_5 was restored by the substitution of $DNal^5$ and $DNal^{12}$, but the affinity for sst_2 again dropped as did the antagonist activity (**25**, DC-38-64 IC_{50} 375 nM). However, the substitution of $DNal^5$ with Nal^{12} caused a dramatic reduction in antagonism (**26**, NC-8-61) to 180 μM. The reversal of the cystine bridge chirality again caused a loss of antagonism and a reduction in binding affinity (**27**, DC-32-53). Trp^5 caused an increase in antagonism relative to its Nal^5 parent (**28**, DC-38-70, vs **24**, DC-38-67) although its affinity for sst_2 was halved, but its sst_3 and sst_5 affinities were much improved. The bulky aromatic residue Bip^5 (29, JF-04-47) caused a doubling in the antagonist IC_{50} relative to Nal^5, but neither compound was particularly potent nor selective. Additionally, the substitution of the carboxyl terminal Nal by the smaller hydrophobic isopropylamide moiety led to a partial antagonist with poor affinity for the sst receptors (**30**, RJ-01-14).

Investigations of the effect of changes in the critical β-bend region, again by replacing the Tyr^7 residue, retained the antagonist activity and in some cases improved the potencies markedly. Using the $DNal^5$ Nal^{12} agonist BIM-23042 as a starting structure, the

substitution of His^7, with the putative antagonist chiral inversion, caused a reduction in antagonism and affinity (**31**, RJ-01-20) relative to the parent compound (**21**, DC-38-39), but replacement with Pal^7 (**32**, DC-38-48) was associated with a 5-fold increase in the antagonist potency to 15.1 nM, although the affinity for sst_2 was halved. Replacement of Nal^5 in this analogue with Phe^5 (**33**, DC-38-51) was accompanied by a reduction in antagonism and affinity for sst_2. Similarly, substitution with the bulky amino acid Dip in position 5 (**34**, RJ-01-28) caused a partial loss of antagonistic potency and a marked lowering of sst_2 affinity, though with a small increase in sst_5 affinity. These reductions were further enhanced by the inversion of the chirality of Dip^5 (**35**, RJ-01-44). The double substitution of Dip in positions 5 and 12 with Pal^7 (**36**, RJ-01-76) caused a marked lowering in antagonism to 500 nM. Again, the substitution of Pal^7 with His^7 led to a further reduction in antagonism (**37**, RJ-01-31; 975 nM). The combination of Dip^5,His^7,Nal^{12} in this analogue produced a weak antagonist (**38**, RJ-01-36), as did Nal^5,His^7,$^D Dip^{12}$ (**39**, RJ-01-40). However, the Nal^5,Pal^7,Dip^{12} analogue (**40**, RJ-01-80) had an IC_{50} of 56.3 nM with an sst_2 affinity of 397 nM.

Cyclic Octapeptides. The recently discovered cyclic 5-12 octapeptide analogue BIM-23068 is highly selective for sst_5. However, inverting the chirality of the cysteine bridge with either one (**41**, DC-37-57) or two (**42**, DC-37-83) DCys residues did not induce antagonism at the doses investigated in the predominately sst_2-mediated antagonist assay.[5]

Since the presence of Pal in position 7 led to the most potent antagonist reported here (compound **32**, DC-38-48; IC_{50} 15.1 nM), we tried this substitution in an antagonist sequence reported by Bass: H-Npa-cyclo-[DCys-Tyr-DTrp-Lys-Val-Cys]-Tyr-NH_2. The Pal^7 analogue (43, JF-04-33) was also an antagonist with an IC_{50} of 26.5 nM and was selective for sst_2 with a K_i of 35.3 nM, compared with the Tyr^7 analogue (44, JF-04-27; IC_{50} 50.0 nM, sst_2 K_i 23.4 nM, sst_5 K_i 101 nM). In comparing these somatostatin antagonists with the compounds reported recently by Bass and co-workers, it should be noted that the above-published antagonist sequence of Bass et al. (H-Npa-cyclo[DCys-Pal-DTrp-Lys-Val-Cys]-Tyr-NH_2 (**44**)) while selective for sst_2 is not as potent in our assay systems, with an IC_{50} of 50 nM and binding affinities of 23 and 101 nM for human sst_2 and sst_5, respectively, as previously reported.[28] It is interesting to observe that the most potent antagonist reported by Bass had an acetylated amino terminus. In this work, we found that acetylation of analogue **21** to give Ac-Nal-cyclo[DCys-Tyr-DTrp-Lys-Val-Cys]-Nal-NH_2 (**22**) was accompanied by 2-fold increases in affinity for sst_1 and sst_5 with slight decreases in the IC_{50} and affinity for sst_2 together with a marked decrease in solubility.

The above data clearly demonstrate a different structure−activity relationship for the agonists compared with the antagonist analogues. Both series of analogues are represented by the cyclic hexapeptides with two pendant extracyclic amino acids. The preferred configuration for these octapeptide agonists consists of a hydrophobic amino acid in position 5 in the D configuration, with the amino acid in position 12 in the L configuration; the disulfide bridge residues in the L configuration and is exemplified by BIM-23014 (Lanreotide/Somatuline). From the present compounds, the antagonists clearly prefer both pendant amino acids in the L configuration (positions 5 and 12), with the disulfide bridge in the D^6, L^{11} configuration. This is illustrated by comparison of the various configurations of the Nal^5, Tyr^7, Nal^{12} antagonists (compounds **21**, **24**, **23**, and **25**: L−L, L−D, D−L, and D−D, respectively). The IC_{50} drops from a high of 35.3 nM for the L−L analogue to a low of 1363 nM for the D−L analogue. This trend is also shown by the Dip^5, Nal^{12} analogues (analogues **34**, L−L, and **35**, D−L; IC_{50} 67 and 335 nM, respectively) and the Phe^5, Thr^{12} analogues (compounds **18**, L−L; IC_{50} 905 nM, and **19**, D−L; inactive). This same trend is also illustrated by the Thr^{12} linear analogues, though with much reduced potencies; again the L−L linear analogue was marginally more active than the D−L analogue (**7**; 3.03 μM; and **6**; 3.96 μM) in the antagonism assay. Additionally, these data suggest that a hydrophobic amino acid is preferred in position 12 and Pal^7 is preferred over Tyr^7.

Three-Dimensional Model of the Antagonists. Recently, we published a paper on the three-dimensional quantitative structure−activity relationships (3-D QSAR) of the somatostatin agonists.[29] It describes two conformational models of somatostatin based on information from NMR experiments.[21,30] Although both conformational models gave highly significant cross-validated r^2's (q^2) based on the training set of molecules, only one gave useful predictions for the bioactivity of novel compounds not included in the training set. Model A, based on NMR conformational data of Van Binst and Tourwé,[21] produced an excellent quantitative model for the GH release-inhibiting activity of the analogues, with a highly predictive r^2. This conformational model for somatostatin is also sterically consistent with this new series of antagonists, which share many of the same structural features with the agonists. The other agonist conformational models, based on the data of He et al.,[31] were not amenable to model the antagonists due to severe intramolecular steric collisions upon the inversion of the chirality of Cys^6. Figure 1 shows the superimposition of various configurations of the Nal^5, Tyr^7, Nal^{12} antagonists (L−L, L−D, D−L, and D−D: compounds **21**, **24**, **23** and **25**, respectively) on the structurally similar agonist BIM-23042. All compounds were built as described in the Experimental Section in the conformation of model A[30] and superimposed by an rms fit of the heavy backbone atoms of the common Tyr^7-Val^{10} sequence to the agonist (see Figure 1). For clarity, only the conformationally variable bridging regions of the antagonists are shown. As can be seen from Figure 1, the inversion of the chirality of Cys in position 6 to form an antagonist causes the *N*-terminal pendant amino acid to be placed on the other side of the molecule relative to the agonist. Changes in the chirality of the *N*-terminal amino acid can be accommodated with only a change in the orientation of the amino group itself.

The three-dimensional structures of the sst receptors have not been definitively determined. Bacteriorhodopsin is one of the few seven-helix transmembrane receptors partially characterized by crystallography and

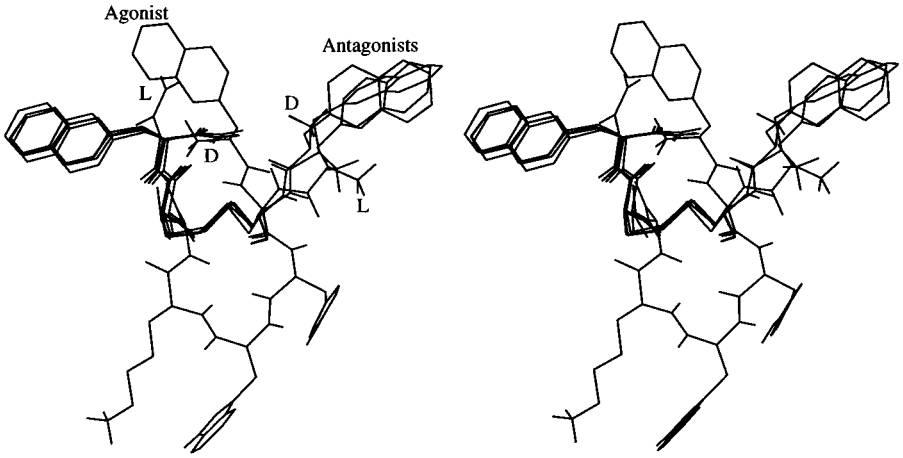

Figure 1. Three-dimensional stereopair showing an agonist (BIM-23042) with the superimposition of similar DCys[6] antagonist isomers (compounds **21**−**24**), differing only in chirality of the exocyclic amino acids. The antagonists were superimposed by an rms fit of the heavy backbone atoms of the common Tyr[7]-Val[10] sequences to the agonist backbone. For clarity, only the full structure of the agonist is shown.

electron diffraction.[31] The relative placement of the helices of bacteriorhodopsin was determined within the resolution of ≥3.5 Å, but no information was deduced concerning the critical intra- and extracellular loop regions. In a recent paper describing a putative interaction between the somatostatin agonists and the sst_2 receptor, the authors derived a simplified model for the ligand bound to the receptor.[32] The model was constructed using the coordinates of bacteriorhodopsin as a template for the alignment of the helical domains of sst_2, despite a lack of homology between bacteriorhodopsin and the sst receptors. No loops or termini were added to the helical domains in this model.

Binding of the agonists in this model was primarily mediated by an interaction between Lys[9] of the ligand and Asp[122] in the third transmembrane helical region of the receptor. The extra- and intracellular loops and the terminal regions of the sst receptors are less highly conserved than the transmembrane helices[3] and presumably are conformationally more mobile since they are beyond the viscous constraints of the membrane bilayer. Assuming a similar binding mode for the antagonists as the agonists, this model would place the pendant, exocyclic amino acids of this current series within the interface of the transmembrane helices and the extracellular loops. The current somatostatin agonist and antagonist series are dominated by large hydrophobic residues in the extracyclic positions, particularly at the N-terminus, with more variability tolerated at the C-terminus. Since the antagonists have an inverted chiral center in the disulfide bridge placing the N-terminal residue in a different orientation relative to the agonists, they are presumably interacting with different hydrophobic domains within the extracyclic loop interface of the receptor.

Currently, we are extending the prior 3-D QSAR of somatostatin agonists to the antagonists and further exploring the antagonist paradigm to increase affinities for cloned human and rat sst_2 receptors and to increase the in vitro potency of the analogues in the rat model. We are also investigating the dynamics of the ligand−receptor interaction in an attempt to model this interaction, computationally.

Experimental Section

Abbreviations. Abbreviations of the common amino acids are in accordance with the recommendations of IUPAC−IUB.[33] Additional abbreviations: Abu, 2-aminobutyric acid; Ahp, 7-aminoheptanoic acid; Bip, biphenylalanine; Cpa, 4-chlorophenylalanine; Dip, 3,3-diphenylalanine; Nal, 3-(2-naphthyl)alanine; Npa, 4-nitrophenylalanine; Pal, 3-pyridylalanine; Pen, penicillamine.

Materials. 4-Methylbenzhydrylamine hydrochloride resin (0.41 or 0.29 mequiv g^{-1}) was obtained from Advanced ChemTech Inc., Louisville, KY. N^{α}-*tert*-Butyloxycarbonyl (Boc)-protected amino acids were purchased from Bachem Inc., Torrance, CA, Advanced ChemTech Inc., and Synthetech Inc., Albany, OR. The reactive side chains of the amino acids were masked with one of the following groups: Cys, 4-methylbenzyloxycarbonyl; His, 3-Bom; Lys, 2-chlorobenzyloxycarbonyl; Ser and Thr, *O*-benzyl; Tyr, *O*-2,6-dichlorobenzyl. All reagents and solvents were ACS grade or better and used without further purification.

Peptide Synthesis. The somatostatin antagonists were assembled on 4-methylbenzhydrylamine-functionalized, 1% cross-linked polystyrene resin (0.29 or 0.41 mequiv g^{-1}) in 0.25 or 0.5-mmol scale on CS Bio Co. (San Carlos, CA; model no. CS 136) or Advanced ChemTech (model 200) synthesizers, using the following protocol: deblocking, 40% TFA (5 min, 19 min); DCM wash cycle (three washes); neutralization, 10% DIEA (1 min, 5 min); DMF wash cycle; DCM wash cycle (two washes); double coupling; first with 1,3-diisopropylcarbodiimide esters (3 equiv), 30 min in DCM; DCM wash (three washes); second coupling with preformed TBTU esters (3 equiv), 90 min in DMF, with a catalytic amount of DIEA; DMF wash (one wash); DCM wash (three washes). Coupling reactions were monitored qualitatively with the ninhydrin test. The crude peptides were cleaved and deprotected with anhydrous hydrogen fluoride (45 min) at 0 °C. RJ-01-48 was synthesized using Boc-Lys(Fmoc). The protected peptide was cleaved from Merrifield resin by HF, cyclized with DCC/HOBt in DMF (∼500 mL) for 3 h, and deprotected with 20% piperidine for 4 h.

Peptide Cleavage. The peptides were cleaved from the resin support with simultaneous side-chain deprotection by acidolysis using anhydrous hydrogen fluoride containing anisole (∼30%, v/v) and dithiothreitol (∼0.6%, w/v) as scavengers for 45 min at 0 °C. Cysteine-containing peptides were cyclized in 90% acetic acid (∼500 mL) with a slight excess of I_2 (15 min). Excess I_2 was then removed by the addition of ascorbic acid.

Purification. The crude peptides were purified by preparative RP-HPLC on C18 bonded silica gel using axial

compression columns (Dynamax-300 Å, 5 or 8 μm, 21.4 × 250 mm). A linear gradient elution system at a flow rate of 20 mL min^{-1} was employed: A, 0.1% TFA; B, 0.1% TFA in 80% MeCN; 20% B to 50% B at 1% min^{-1}. The separations were monitored at 280 nm, by TLC on silica gel plates (Merck F60) and by analytical RP-HPLC. The fractions containing the product were pooled, concentrated in vacuo, and subjected to lyophilization. Each peptide was obtained as a fluffy white powder of constant weight by lyophilization from aqueous acetic acid. The purity of the final peptides was assessed by analytical RP-HPLC in two systems. Analytical RP-HPLCs were recorded using a Vydac C18 support (4.6 × 250 mm, 5 μm, 300-Å pore size; Liquid Separations Group). The two linear gradient systems were used at a flow rate of 1.5 mL min^{-1}: HPLC-1, A, 0.1% TFA; B, 0.1% TFA in 80% MeCN; 10% B to 70% B at 1% min^{-1}; and HPLC-2, C, 5% MeCN in TEAP (0.1 M, pH 3); D, 20% C in MeCN 0% D to 60% D at 1% min^{-1}. Column eluent was monitored at 215 nm. The retention time and purity of each peptide was assessed by the Rainin Dynamax HPLC Method Manager. The results are given in Table 2.

Amino Acid Analysis. The peptides were hydrolyzed in vacuo (110 °C, 20 h) in 4 M methanesulfonic acid containing 0.2% 3-(2-aminoethyl)indole (Pierce). Amino acid analyses were performed on the hydrolysates following derivatization with *o*-phthaldialdehyde reagent (Sigma Chemical Co.) using an automatic HPLC system (Rainin Instrument Co.) fitted with a 100 × 4.6 mm, 3 μm C18 axial compression column with integral guard column (Microsorb AAAnalysis, Type O; Rainin Instrument Co.). The derivatized primary amino acids were eluted using a binary gradient of buffer A, 0.05 M sodium acetate containing 4.5% (v/v) methanol and 0.5% (v/v) tetrahydrofuran at pH 7.2, and buffer B, methanol. The gradient sequence—0% A at 0 min, 35% A at 16.5 min, 90% A at 30 min, and 90% A at 33 min—was used with a flow rate of 1.0 mL min^{-1} at ambient temperature. Eluent was monitored at 340 nm and integrated by the Dynamax Method Manager (Rainin Instrument Co.). Standard retention times were as follows: Asp, 6.6 min; Arg, 19.9 min; Trp, 25.4 min; and Lys, 29.5 min. Each peptide produced the expected results within the error range of ±10% (results not shown).

Mass Spectrometry. The peptides were analyzed by matrix-assisted laser desorption/ionization time-of-flight mass spectrometry using a LaserMat 2000 mass spectrometer (Finnigan MAT, San Jose, CA) using α-cyano-4-hydroxycinnamic acid as the matrix with substance P (1348.7 Da) as an internal standard. In each case, the spectra consisted of a major M − H$^+$ ion peak for the internal standard, the expected analyte M − H$^+$ peak, and a few peaks associated with the matrix (<500 Da). The results are given in Table 2.

Antagonism of the *in Vitro* SRIF Inhibition of GH Release. Anterior pituitaries from adult male rats were collected and dispersed by a previously described trypsin/DNase method.[34] The dispersed cells were diluted with sterile-filtered Dulbecco's modified Eagle medium (MEM; Gibco Laboratories, Grand Island, NY), which was supplemented with 2.5% fetal calf serum (Gibco), 3% horse serum (Gibco), 10% fresh rat serum (stored on ice for no longer than 1 h) from the pituitary donors, 1% MEM nonessential amino acids (Gibco), gentamycin (10 ng mL^{-1}; Sigma), and nystatin (10 000 U mL^{-1}; Gibco). The cells were randomly plated at a density of approximately 200 000 cells/well (Costar cluster 24; Rochester Scientific Co., Rochester, NY). The plated cells were maintained in the above Dulbecco's medium in a humidified atmosphere of 95% air and 5% CO_2 at 37 °C for 4−5 days. In preparation for a hormone challenge, the cells were washed with medium 199 (Gibco; 3 × 1 mL). Each dose of analogue (6 total/plate) was tested in the presence of SRIF (1 nM) in triplicate wells in a total volume of 1 mL of medium 199 containing 1% BSA (fraction V; Sigma Chemical Co.). All wells contained GHRH(1−29)NH_2 (1 nM). A GHRH(1−29)NH_2 (1 nM)-stimulated control group and an SRIF (1 nM) with GHRH(1−29)NH_2 (1 nM)-inhibited control group were included on each cell culture plate. After incubation in an air/carbon dioxide atmosphere (95/5%, 3 h at 37 °C), the medium was removed and stored at −20 °C until assayed for hormone content. Growth hormone in media was measured by a standard double-antibody RIA using components generously supplied by the NHPP, NIDDK, NICHHD, and USDA. Antagonist IC_{50}'s versus IC_{50} of SRIF (1 nM) were calculated using Sigmaplot (Jandel Scientific, San Rafael, CA). Values are expressed as the mean IC_{50} (nM) ± SEM from (*n*) separate dose−response curves.

Functional Expression of the Cloned Human Somatostatin Receptors. The genomic clones containing the human somatostatin receptors ($hsst_{1-5}$)[35−39] were kindly provided by Dr. Graeme I. Bell (University of Chicago). The $hsst_1$, $hsst_2$, $hsst_3$, $hsst_4$, and $hsst_5$ cDNAs were isolated as a 1.5-kb *Pst*I-*Xmn*I fragment, 1.7-kb *Bam*HI-*Hin*dIII fragment, 2.0-kb *Nco*I-*Hin*dIII fragment, 1.4-kb *Nhe*I-*Nde*I fragment, and 1.2-kb *Hin*dIII-*Xba*I fragment, respectively, each containing the entire coding region of the full-length receptors. These fragments were independently subcloned into the corresponding restriction endonuclease sites in the mammalian expression vector pCMV5, downstream from the human cytomegalovirus (CMV) promoter, to produce the expression plasmids pCMV5/$hsst_1$, pCMV5/$hsst_2$, pCMV5/$hsst_3$, pCMV5/$hsst_4$, and pCMV5/$hsst_5$. For transfection into CHO-K1 cells, a plasmid, pRSV-neo (American Type Culture Collection, Rockville, MD), carrying the neomycin mammalian cell-selectable marker was added.

Receptor Expression and Transfection. Transfections were performed by the calcium phosphate method. CHO-K1 cells were maintained in α-minimum essential medium (α-MEM; Gibco) supplemented with 10% fetal calf serum and transfected with each of the expression plasmids using calcium phosphate precipitation. Clones that had inherited the expression plasmid were selected in α-MEM supplemented with 500 μg mL^{-1} geneticin (G418; Gibco). Independent CHO-K1 clones were picked by glass-ring cloning and expanded in culture in the selective media. Membranes were prepared from the isolated clones, and hsst expression was initially assessed for binding with [^{125}I]SRIF-14 and [^{125}I]MK-678 (for sst_2).

Radioligand Binding Assays. Cell membranes of the five cell types were obtained from homogenates (Polytron setting 6, 15 s) of the corresponding CHO-K1 cells, in ice-cold Tris-HCl (50 mM) and centrifuged (39000*g*, 10 min × 2), with an intermediate resuspension in fresh buffer. The final pellets were resuspended in Tris-HCl (10 mM) for assay. Aliquots of the membranes were incubated (30 min at 37 °C) with 0.05 nM [^{125}I]Tyr^{11}-SRIF (types 1, 3, 4, 5) or [^{125}I]MK-678 (type 2) in 50 nM HEPES (pH 7.4) containing BSA (10 mg mL^{-1}), $MgCl_2$ (5 mM), Trasylol (200 kIU mL^{-1}), bacitracin (0.02 mg mL^{-1}), and phenylmethanesulfonyl fluoride (0.02 mg mL^{-1}). The final assay volume was 0.3 mL, and incubations were terminated by rapid filtration through GF/C filters presoaked in 0.3% poly(ethylenimine) using a Brandel rapid filtration module. Each tube and filter was then washed with aliquots of cold buffer (3 × 5 mL). Specific binding was defined as the total radioligand bound minus that bound in the presence of 1.0 μM SRIF.

Molecular Modeling. All molecular modeling was performed on a Silicon Graphics Indigo^2 High Impact 10000 computer, using SYBYL 6.32[40] with the standard TRIPOS force field,[41] as described previously.[30] The agonist conformation model (model A)[30] was based on the NMR conformational inferences of Van Binst and Tourwé.[21] The initial compound BIM-23034 (DPhe^5-cyclo[Cys^6-Tyr^7-DTrp^8-Lys^9-Val^{10}-Cys^{11}]-Nal^{12}-NH_2) was built from the predefined amino acids and its conformation set to β-sheet. The type II′ bend was introduced around DTrp^8-Lys^9 and the cysteine bridge formed. Partial atomic charges were calculated for the molecule with a charged amino terminus using the Pullman method.[42,43] The geometries of the exocyclic residues, DPhe^5 and Nal^{12}, were adjusted visually to facilitate hydrogen bond formation between DPhe^5-CO and Nal^{12}NH.[21] The structure was then optimized by energy minimization using the Broyden, Fletcher, Goldfarb, and Shannon (BFGS) algorithm to a final root-mean-square

(rms) gradient of ≤0.1 kcal mol Å^{-1}. A distance-dependent dielectric function[44] was employed together with the default settings for all the other minimization options. Mutation of this analogue by substitution of the amino acids of the agonist (BIM-23042, H-D-Nal[5]-cyclo[Cys[6]-Tyr[7]-D-Trp[8]-Lys[9]-Val[10]-Cys[11]]-Nal[12]-NH_2)[30] and reminimization gave the conformation shown in Figure 1 (agonist) in which the N and C termini were hydrogen bonded. The Nal[5], Tyr[7], Nal[12] antagonists based on the same amino acid composition (compounds **21**, **24**, **23** and **25**: L−L, L−D, D−L and D−D, respectively) were derived from this model by the inversion of the chirality of Cys[6] and appropriate inversion of the chirality of the pendant amino acids. These were minimized as before and superimposed on the agonist by an rms fit of the heavy backbone atoms of the common Tyr[7]-Val[10] sequences. Figure 1 shows the entire agonist with the four antagonists superimposed. For clarity, only the conformationally variable bridging region of the antagonists is shown.

Acknowledgment. We would like to thank Ms. Etchie Yauger for her excellent support of this work in performing the purification of many peptides reported herein and amino acid analysis of all the peptides, Dr. Ning-Yi Jiang and Mr. Joseph Fuselier for the synthesis and purification of some of the peptides, Ms. L. Vienna Mackey for her assistance with the in vitro antagonist biological assays, and Ms. Karyn Van Buren for her expeditious administrative support.

References

(1) Brazeau, P.; Vale, W.; Burgus, R.; Ling, N.; Butcher, M.; Rivier, J.; Guillemin, R. Hypothalamic Polypeptide that Inhibits the Secretion of Immunoreactive Pituitary Growth Hormone. *Science* **1973**, *179*, 77−79.

(2) Reisine, T.; Bell, G. I. Molecular Properties of Somatostatin Receptors. *Neuroscience* **1995**, *67*, 777−790.

(3) Reisine, T.; Bell, G. I. Molecular Biology of Somatostatin Receptors. *Endocrine Rev.* **1995**, *16*, 427−442.

(4) Coy, D. H.; Taylor, J. E. Receptor-Specific Somatostatin Analogues: Correlations with Biological Activity. *Metabolism* **1996**, *34* (Suppl. 1), 21−23.

(5) Raynor, K.; Murphy, W. A.; Coy, D. H.; Taylor, J. E.; Moreau, J.-P.; Yasuda, K.; Bell, G. I.; Reisine, T. Cloned Somatostatin Receptors: Identification of Subtype-Selective Peptides and Demonstration of High Affinity Binding of Linear Peptides. *Mol. Pharmacol.* **1993**, *43*, 838−844.

(6) Rossowski, W. J.; Coy, D. H. Specific Inhibition of Rat Pancreatic Insulin and Glucagon Release by Receptor-Selective Somatostatin Analogues. *Biochem. Biophys. Res. Commun.* **1994**, *205*, 341−346.

(7) Rossowski, W. J.; Gu, Z. F.; Akarca, U. S.; Jensen, R. T.; Coy, D. H. Characterization of Somatostatin Receptor Subtypes Controlling Rat Gastric Acid and Pancreatic Amylase Release. *Peptides* **1994**, *15*, 1421−1424.

(8) Murthy, K. S.; Coy, D. H.; Makhlouf, G. M. Somatostatin Receptor-Mediated Signaling in Smooth Muscle − Activation of Phospholipase C-β3 by Gβgamma and Inhibition of Adenyl Cyclase by GαiIGαo. *J. Biol. Chem.* **1996**, *271*, 23458−23463.

(9) Fries, J. L.; Murphy, W. A.; Sueiras-Diaz, J.; Coy, D. H. Somatostatin Antagonist Analogue Increases GH, Insulin and Glucagon Release in the Rat. *Peptides* **1982**, *3*, 811−814.

(10) Spencer, G. S. G.; Hallett, K. G. Somatostatin Antagonist Analogue Stimulates Growth in Rats. *Life Sci.* **1985**, *37*, 27−30.

(11) Bass, R. T.; Buckwalter, B. L.; Patel, B. P.; Pausch, M. H.; Price, L. A.; Strnad, J.; Hadcock, J. R. Identification and Characterization of Novel Somatostatin Antagonists. *Mol. Pharmacol.* **1996**, *50*, 709−715.

(12) Bass, R. T.; Buckwalter, B. L.; Patel, B. P.; Pausch, M. H.; Price, L. A.; Strnad, J.; Hadcock, J. R. Identification and Characterization of Novel Somatostatin Antagonists, Erratum. *Mol. Pharmacol.* **1997**, *51*, 170.

(13) Veber, D. F.; Holly, F. W.; Nutt, R. F.; Bergstrand, S. J.; Brady, S. F.; Hirschmann, R. Highly Active Cyclic and Bicyclic Somatostatin Analogues of Reduced Ring Size. *Nature* **1979**, *280*, 512−514.

(14) Nutt, R. F.; Veber, D. F.; Curley, P. E.; Saperstein, R.; Hirschmann, R. F. Somatostatin Analogues Which Define the Role of the Lysine-9 Amino Group. *Int. J. Pep. Protein Res.* **1983**, *21*, 66−73.

(15) Nutt, R. F.; Saperstein, R.; Veber, D. F. Structural and Conformational Studies Regarding Tryptophan in a Cyclic Hexapeptide Somatostatin Analogue. In *Peptides: Chemistry and Biology, Proceedings of the Eighth American Peptide Symposium*; Hruby, V. J., Rich, D. H., Eds.; Pierce Chemical Co.: Rockford, IL, 1983; pp 345−348.

(16) Veber, D. F. Design and Discovery in the Development of Peptide Analogues. In *Peptides: Chemistry and Biology, Proceedings of the Twelfth American Peptide Symposium*; Smith, J. A., Rivier, J. E., Eds.; ESCOM: Leiden, 1992; pp 3−14.

(17) Ösapay, G.; Prokai, L.; Ho-Seung, K.; Medzihradszky, K. F.; Coy, D. H.; Liapakis, G.; Reisine, T.; Melacini, G.; Zhu, Q.; Wang, S. H.-H.; Mattern, R.-H.; Goodman, M. Lanthionine-Somatostatin Analogues: Synthesis, Characterizatin, Biological Activity, and Enzymatic Stability Studies. *J. Med. Chem.* **1997**, *40*, 2241−2251.

(18) Freidinger, R. M.; Schwenk Perlow, D.; Randall, W. C.; Saperstein, R.; Arison, B. H.; Veber, D. F. Conformational Modifications of Cyclic Hexapeptide Somatostatin Analogues. *Int. J. Pept. Protein Res.* **1984**, *23*, 142−150.

(19) Chen, L.; Skinner, S. R.; Gordon, T. D.; Taylor, J. E.; Barany, G.; Morgan, B. A. Isolation, Characterization and Synthesis of a Trisulfide Related to the Somatostatin Analogue Lanreotide. *Proceedings of the Fifteenth American Peptide Symposium*; 1997; in press.

(20) Thurieau, C.; Janiak, P.; Krantic, S.; Guyard, C.; Pillon, A.; Kucharczyk, N.; Vilaine, J. P.; Fauchere, J. L. A New Somostatin Analogue with Optimized Ring Size Inhibits Neointimal Formation Induced by Balloon Injury in Rats Without Altering Growth Hormone Release. *Eur. J. Med. Chem.* **1995**, *30*, 115−122.

(21) Van Binst, G.; Tourwé, D. Backbone Modifications in Somatostatin Analogues: Relation between Conformation and Activity. *Pept. Res.* **1992**, *5*, 8−13.

(22) All analogues were assayed for antagonist activity in the presence of SRIF-14 at analogue doses up to 10 μM. Some were tested to doses of 100 μM as denoted in Table 3.

(23) Bauer, W.; Briner, U.; Doepfner, W.; Haller, R.; Huguenin, R.; Marbach, P.; Petcher, T. J.; Pless, J. SMS 201-995: A Very Potent and Selective Octapeptide Analogue of Somatostatin with Prolonged Action. *Life Sci.* **1982**, *31*, 1133−1140.

(24) Brady, S. F.; Nutt, R. F.; Holly, F. W.; Paleveda, W. J.; Strachan, R. G.; Bergstrand, S. J.; Veber, D. F.; Saperstein, R. Synthesis and Biological Activity of Somatostatin Analogues of Reduced Ring Size. In *Peptides: Synthesis, Structure, Function. Proceedings of the Seventh American Peptide Symposium*; Rich, D. H., Gross, E., Eds.; Pierce Chemical Co.: New York, 1981; pp 653−656.

(25) Veber, D. F. Design and Discovery in the Development of Peptide Analogues. In *Peptides: Chemistry and Biology. Proceedings of the Twelfth American Peptide Symposium*; Smith, J. A., Rivier, J. E., Eds.; ESCOM: Leiden, 1992; pp 3−14.

(26) Patel, Y. C.; Srikant, C. B. Subtype Selectivity of Peptide Analogues for all five Cloned Human Somatostatin Receptors. *Endocrinology* **1994**, *135*, 2814−2817.

(27) Folkers, K.; Bowers, C. Y.; Kubiak, T.; Stepinski, J. Antagonists of the Luteinizing Hormone Releasing Hormone with Pyridyl-Alanines which Completely Inhibit Ovulation at Nanogram Dosage. *Biochem. Biophys. Res. Commun.* **1983**, *3*, 1089−1095.

(28) Orbuch, M.; Taylor, J. E.; Coy, D. H.; Mrozinski, J. E.; Mantey, S.; Battey, J. F.; Moreau, J.-P.; Jensen, J. T. Discovery of a Novel Class of Neuromedin B Receptor Antagonists, Substituted Somatostatin Analogues. *Mol. Pharmacol.* **1993**, *44*, 841−850.

(29) Coy, D. H.; Murphy, W. A.; Rossowski, W. J.; Hocart, S. J.; Jain, R.; Fuselier, J.; Taylor, J. E. Somatostatin Receptor Antagonists Based on a Mixed Neuromedin B Antagonist/Somatostatin Agonist. *Proceedings of the Fifteenth American Peptide Symposium*; 1997; in press.

(30) Hocart, S. J.; Reddy, V.; Murphy, W. A.; Coy, D. H. Three-Dimensional Quantitative Structure Activity Relationships (3-D QSAR) of Somatostatin Analogues. I. Comparative Molecular Field Analysis (CoMFA) of Growth Hormone Release-Inhibiting Potencies. *J. Med. Chem.* **1995**, *38*, 1974−1989.

(31) He, Y.-A.; Huang, Z.; Raynor, K.; Reisine, T.; Goodman, M. Syntheses and Conformations of Somatostatin-Related Cyclic Hexapeptides Incorporating Specific α- and β-Methylated Residues. *J. Am. Chem. Soc.* **1993**, *115*, 8066−8072.

(32) Henderson, R.; Baldwin, J. M.; Ceska, T. A.; Zemlin, F.; Beckmann, E.; Downing, K. H. Model for the Structure of Bacteriorhodopsin Based on High-resolution Electron Cryomicroscopy. *J. Mol. Biol.* **1990**, *213*, 899−929.

(33) Kaupmann, K.; Bruns, C.; Raulf, F.; Weber, H. P.; Mattes, H.; Lübbert, H. Two Amino Acids Located in Transmembrane Domains VI and VII, Determine the Selectivity of the Peptide Agonist SMS 201-995 for the SSTR2 Somatostatin Receptor. *EMBO J.* **1995**, *14*, 727−735.

(34) IUPAC−IUB Commission of Biochemical Nomenclature (CBN) Symbols for Amino-Acid Derivatives and Peptides, Recommendations 1971. *Eur. J. Biochem.* **1972**, *27*, 201−207.

(35) Murphy, W. A.; Taylor, J.; Moreau, J.-P.; Coy, D. H. Novel Heptapeptide Somatostatin Analogue Displays Antitumor Activity Independent of Effects on Growth Hormone Secretion. *Pept. Res.* **1989**, *2*, 128−132.
(36) Yamada, Y.; Post, S. R.; Wang, K.; Tager, H. S.; Bell, G. I.; Seino, S. Cloning and Functional Characterization of a Family of Human and Mouse Somatostatin Receptors Expressed in Brain, Gastrointestinal Tract and Kidney. *Proc. Natl. Acad. Sci. U.S.A.* **1992,** *89*, 251−255.
(37) Yasuda, K.; Rens-Domiano, S.; Breder, C. D.; Law, S. F.; Sapel, C. B.; Reisine, T.; Bell, G. I. Cloning of a Novel Somatostatin Receptor, SSTR-3, Coupled to Adenyl Cyclase. *J. Biol. Chem.* **1992**, *267*, 20422−20428.
(38) Yamada, Y.; Reisine, T.; Law, S. F.; Ihara, Y.; Kubota, A.; Kagimoto, S.; Seino, M.; Seino, Y.; Bell, G. I.; Seino, S. Somatostatin Receptors, an Expanding Gene Family: Cloning and Functional Characterization of Human SSTR3, a Protein Coupled to Adenylate Cyclase. *Mol. Pharmacol.* **1992,** *42*, 2136−2142.
(39) Rohrer, L.; Raulf, F.; Bruns, C.; Buettner, R.; Hofstaedter, F.; Schule, R. Cloning and Characterization of a Fourth Human Somatostatin Receptor. *Proc. Natl. Acad. Sci. U.S.A.* **1993,** *90*, 4196−4200.
(40) O'Carroll, A. M.; Raynor, K.; Lolait, S. J.; Reisine, T. Characterization of Cloned Human Somatostatin Receptor SSTR5. *Mol. Pharmacol.* **1994**, *46*, 291−298.
(41) SYBYL molecular modeling software, version 6.32; Tripos Associates Inc., 1699 Hanley Rd, St. Louis, MO 63144-2913.
(42) Clark, M.; Cramer, R. D., III; Van Opdenbosh, N. Validation of the General Purpose Tripos 5.2 Force Field. *J. Comput. Chem.* **1989**, *10*, 982−1012.
(43) Berthod, H.; Pullman, A. Calculation of the σ Structure of Conjugated Molecules. *J. Chem. Phys.* **1965**, *62*, 942−946.
(44) Berthod, H.; Prettre, C. G.; Pullman, A. Role of σ and π Electrons on the Properties of Halogens-Substituted Conjugated Molecules. Application to the Study of Uracil and Fluorouracil. *Theor. Chim. Acta* **1967**, *8*, 212−222.
(45) McCammon, J. A.; Wolynes, P. G.; Karplus, M. Picosecond Dynamics of Tyrosine Side Chains in Proteins. *Biochemistry* **1979**, *18*, 927−942.

JM970730Q